CARBON letters

Original Articles
Carbon Letters Vol. 19, 40-46 (2016)

Study on urea precursor effect on the electroactivities of nitrogen-doped graphene nanosheets electrodes for lithium cells

Ki-Yong Kim[1], Yongju Jung[2] and Seok Kim[1,♠]

[1]School of Chemical and Biochemical Engineering, Pusan National University, Busan 46241, Korea
[2]Department of Chemical Engineering, Korea University of Technology and Education, Cheonan 31253, Korea

Article Info

Received 14 November 2015
Accepted 1 April 2016

♠Corresponding Author
E-mail: seokkim@pusan.ac.kr
Tel: +82-51-510-3874

Open Access

DOI: http://dx.doi.org/10.5714/CL.2016.19.040

http://carbonlett.org

pISSN: 1976-4251
eISSN: 2233-4998

Abstract

Nitrogen-atom doped graphene oxide was considered to prevent the dissolution of polysulfide and to guarantee the enhanced redox reaction of sulfur for good cycle performance of lithium sulfur cells. In this study, we used urea as a nitrogen source due to its low cost and easy preparation. To find the optimum urea content, we tested three different ratios of urea to graphene oxide. The morphology of the composites was examined by field emission scanning electron microscope. Functional groups and bonding characterization were measured by X-ray photoelectron spectroscopy. Electrochemical properties were characterized by cyclic voltammetry in an organic electrolyte solution. Compared with thermally reduced graphene/sulfur (S) composite, nitrogen-doped graphene/S composites showed higher electroactivity and more stable capacity retention.

Key words: graphene nanosheets, composite electrodes, lithium cells, N-doping, urea precursor

1. Introduction

Since its invention, the lithium-ion battery has gone through several advancements during its commercialization and application as energy source for a variety of devices. According to use, many improvements were performed and this accelerated the rapid spread of smart devices. In the case of electric vehicles or energy storage system (ESS) for smart grids, an additional development of the lithium-ion battery is required [1-3]. For example, as batteries for electric vehicles, 500 km driving on a single charge is required for full commercialization, which corresponds to energy density of 700 Wh kg^{-1}. However, this is hard to realize because the lithium-ion battery appears to have reached the limits of its development. To solve this problem, researchers have tried to discover a next-generation secondary battery. Among many candidates undergoing intensive research, the lithium-sulfur (Li-S) battery has unusually high specific energy density (2600 Wh kg^{-1}) and high theoretical capacity (1675 mAh g^{-1}) [4-6]. A Li-S battery not only has electrochemical advantages, but also lower price because elemental sulfur is abundant in the environment and could get easily be provided as a by-product of existing industrialization. However, before it could replace the lithium-ion battery, several technical challenges must be met that now hamper commercialization of the Li-S battery. The poor conductivity of pristine sulfur, dissolution of polysulfide into the electrolyte [7-9], and its large volume change (>80%) during the charge/discharge process must be overcome to provide practical application [10]. An alternative way to improve the electric conductivity or stable structure of the needed electrodes would be to use carbon material as a support for the active sulfur material. The high conductivity of carbon can guarantee better electrochemical performance of cells and some carbon has a structure

sufficiently strong to withstand the change in sulfur volume. For these reasons, several forms of carbon were attempted as cathode material supports. Meanwhile, since graphene was detected in 2004, its applications have become widespread [11,12]. Among many fields, ESS has great potential for the adoption of graphene as electrode material because of grapheneldrochemical performance of cell, flexibility, and stability [13-16]. Furthermore, nitrogen-doped graphene sheets (NGS) provide one of the most attractive choices for a Li-S battery due to their excellent adsorption of nitrogen atoms to the carbon matrix [17]. In this regard, nitrogen atoms are of different types depending on their position in a carbon matrix. In detail, pytidicin-N and pyrrolic-N are the main parts that enhance electrochemical performance of energy storage devices. The use of nitrogen atoms in a carbon matrix was expected to prevent dissolution of polysulfide and enhance the cycle performance of cells [18]. Because of its low cost and easy preparation, urea is generally the source of choice for nitrogen doping of graphene-based carbon materials [19,20]. Oxygen-containing functional groups in graphene oxide (GO) and amino-groups of urea are thought to be essential in the formation of C–N bonds in the graphene lattice. Nitrogen-doped graphene has been studied as an electrode material for capacitors and batteries, and as catalyst support for various types of fuel cells. In line with this concept, we tried nitrogen-doped GO from urea precursor, for electrodes of lithium-sulfur cells.

To improve the electrochemical performance of lithium-sulfur cells and to find the optimum content of urea needed to prepare the nitrogen-doped GO, we fabricated three different NGS of varying nitrogen content by facile, thermal, solid-state reaction of GO and urea. After that, a melt-diffusion technique and solution-based synthesis using carbon disulfide (CS_2) were carried out to introduce elemental sulfur between the NGS [21].

2. Experimental

2.1. Materials

Graphite powder (99.9%, 1 ppm mesh) was purchased from Bay Carbon Co., Ltd. (Bay City, MI, USA), and urea was purchased from Yakuri Pure Chemicals Co., Ltd. (Kyoto, Japan). Elemental sulfur and organic solvents were purchased from Sigma-Aldrich. Distilled water was used in all experiments. Li salts and other reagents were used at the guaranteed reagent grade.

2.2. Synthesis of the GO

GO was prepared by Hummer's method. Briefly, a mixture of 1 g of graphite powder and 1 g of sodium nitrate was added to 46 mL of sulfuric acid. After that, 5 g of potassium permanganate was added to the solution and stirred at 35°C for 2 h. Then, 220 mL of H_2O and 5.2 mL of H_2O_2 were added. The oxidized solution was filtered and washed using HCl. The GO obtained was washed again with ethanol and H_2O three times, with centrifugation (3600 r/min, 5 min). GO powder was obtained after freeze drying.

2.3. Synthesis of N-doped graphene sheets

Nitrogen-doped graphene sheets (NGS) were produced by thermal solid-state reaction using urea as the doping source for the prepared GO powder. A mixture of 0.3 g of GO and 0.3, 0.9, and 1.5 g of urea (mass ratio = 1:1, 1:3, 1:5, respectively) were ground in an agate mortar for 30 min; then heat treated in a tube furnace. The samples were designated NGS-1, NGS-2, and NGS-3. Before heat treatment, Ar gas was used to fill the tube furnace for 30 min. Then the temperature was raised to 400°C at a rate of 5°C min^{-1} and kept at the final temperature for 2 h. After cooling to room temperature, the calcined products were filtered and washed using 1 M HCl solution; then dried at 60°C for 12 h. For comparison, we produced thermally reduced graphene (TRG) at 400°C without any nitrogen source.

2.4. Synthesis of NGS/sulfur composites

To insert elemental sulfur between nanosheets, we used a melt-diffusion technique and solution based synthesis with CS_2. First, sulfur was dissolved in CS_2 and stirred for 15 min because sulfur is highly soluble in CS_2 at room temperature. Then, the prepared NGS was added and the solution stirred until the CS_2 solvent fully vaporized. Through this process, sulfur powder was dissolved, moved into position between the nanosheets, and became embedded by their re-crystallization. In order to the sulfur to penetrate effectively, the melt-diffusion technique (in a tube furnace) was carried out consecutively. The mixture was heat treated at 160°C for 12 h under Ar to melt the elemental sulfur and allow it to infiltrate widely. After cooling down to room temperature, the NGS/S composite was obtained.

2.5. Structural characterizations

To investigate the surface morphology of the NGS/S composites, field emission scanning electron microscope (FE-SEM; SUPRA25; Carl Zeiss AG, Oberkochen, Germany) and energy-dispersive X-ray (Raith Elphy Quantum, Dortmund, Germany) were used. We also studied the functional groups and bonding characterization using X-ray photoelectron spectroscopy (XPS; Axis Nova). The sulfur content of the NGS/S composites was calculated based on the thermogravimetric analysis (TGA) data.

2.6. Electrochemical characterization

The electrochemical characterization was determined using a CR-2016 type coin cell. The cathode was prepared by mixing NGS/S composites (80 wt%), Super-P (10 wt%), and polyvinylidene fluoride (10 wt%) in an N-methyl pyrrolidinone. Then, the slurry was spread onto aluminum foil. Test cells consisting of a lithium metal anode, separate, and cathode were assembled in an argon-filled glove box. The electrolyte solution was 1 M lithium bis(trifluoromethane) sulfonamide salt (LITFSI) in a mixture of 1,3-dioxolane (DOL) and 1,2-dimethoxyethane (DME), with a volume ratio of 1:1.

The cycle voltammetry test measurement was conducted with an electrochemical measurement system (WonATech Co., Seoul, Korea). Cyclic voltammetry (CV) was performed in a

voltage range of 1.5–3.0 V, and the scan rate was fixed at 0.2 mV s^{-1}. Charge/discharge cycle tests were conducted using a multichannel high performance battery cycler, between the voltages of 1.5 to 3.0 V at 100 mAh/g.

3. Results and Discussion

To identify the elemental composition of the different NGS composites, XPS measurements were carried out (Fig. 1). All the composites showed an N1s peak, which means that the nitrogen doping by thermal-solid reaction was successful. Two other peaks centered at about 285.0 eV and 531.0 eV, were C1s and O1s, respectively [22]. Table 1 shows the elemental composition and distribution of nitrogen species in the composites. The atomic percent of nitrogen was 12.6% for NGS-1, 16.43% for NGS-2, and 21.96% for NGS-3, which can be attributed to the amounts of nitrogen added. The high

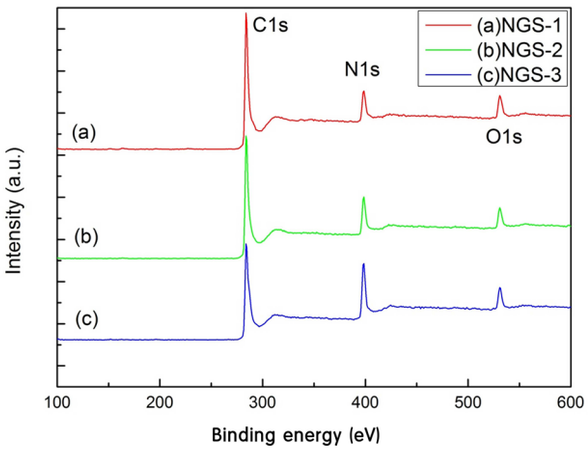

Fig. 1. X-ray photoelectron spectroscopy survey spectra of NGS-1, NGS-2, and NGS-3. NGS, nitrogen-doped graphene.

Table 1. Carbon, nitrogen, oxygen content and N distribution of NGS from XPS measurement

	C at%	N at%	O at%	Pyridinic-N	Pyrrolic-N	Graphitic-N	Pyridine-N-oxide
NGS-1	81.81	12.64	5.55	30.62	68.58	0	0.8
NGS-2	78.04	16.43	5.53	29.99	69.70	0	0.31
NGS-3	72.52	21.96	5.52	28.51	69.88	0	1.6

NGS, nitrogen-doped graphene sheets; XPS, X-ray photoelectron spectroscopy.

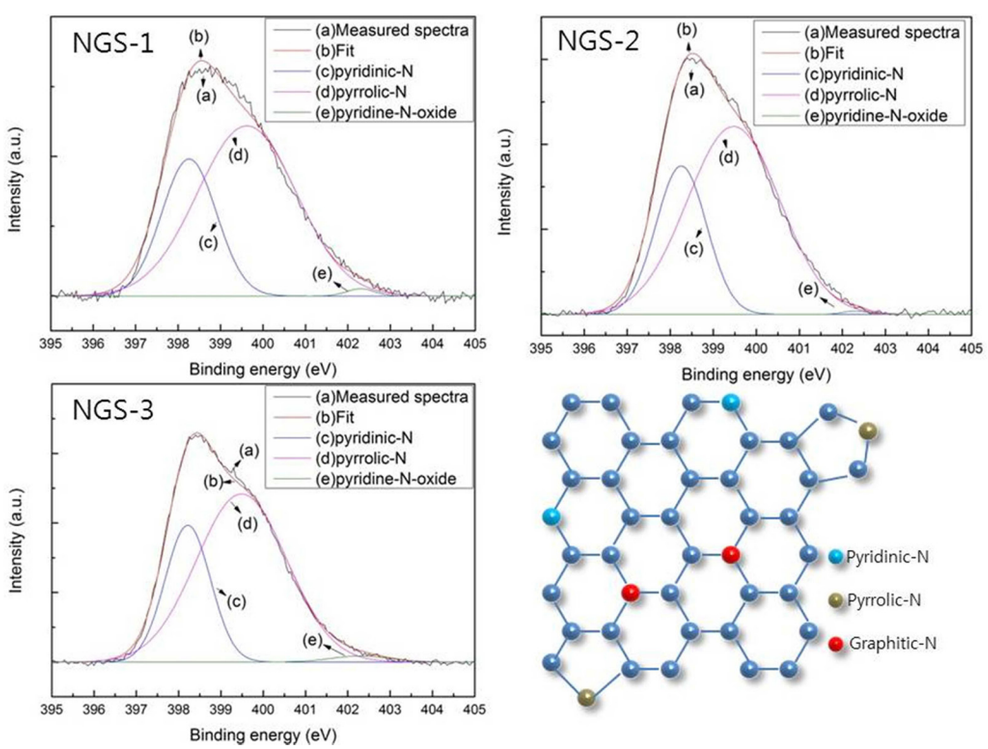

Fig. 2. High resolution N1s X-ray photoelectron spectroscopy spectra of (a) NGS-1, (b) NGS-2, and (c) NGS-3. (d) Schematic model of three types of N-doped graphene: pyridinic-N, pyrrolic-N, and graphitic-N. NGS, nitrogen-doped graphene.

DOI: http://dx.doi.org/10.5714/CL.2016.19.040

resolution N1s peaks of the composites, and the distribution of nitrogen species, are given in Fig. 2. As shown in Table 1, pyrrolic-N was predominant and graphitic-N was not observed for all composites. This was because graphitic-N was probably formed during the thermal solid reaction at 500°C to 700°C [19,23]. The greater amount of nitrogen content in the NGS-3 composite, and the difference in distribution of the nitrogen species, may be dependent on the ratio of urea to GO and would explain the electrochemical performance of the cells [24,25]. The atomic proportions of the nitrogen species were almost proportional to the amounts of urea added to the GO.

The electrochemical performance of the TRG/S, NGS-1/S, NGS-2/S and NGS-3/S composites was tested by CV and galvanostatic charge/discharge measurements. The CV graphs of composite electrodes at 1.5 and 3.0 V for the first cycle, at a scan rate of 0.2 mV s^{-1}, are shown in Fig. 3. All of the composites showed only one oxidation peak, which means that Li_2S_2 and Li_2S were transformed to Li_2S_8. Among the well-defined reduction peaks observed, some indicate the transformation of Li_2S_2 or Li_2S to Li_2S_8; some the reduction of elemental sulfur to high-order lithium polysulfides (e.g., Li_2S_8); then to low-order lithium polysulfides (Li_2S_n, 4 ≤n). Others indicate reduction of lithium polysulfides to solid-states Li_2S_2/Li_2S [26-28]. As shown in Fig. 3, the differences in electrical potential between cathodic and anodic peaks of nitrogen doped samples increased, meaning a large polarization of the electrodes. Moreover, no peaks were observed without the redox reaction peaks of sulfur, indicating that the nitrogen-doped graphene did not have a bad influence on the redox process of sulfur. Fig. 4a and b display CVs of TRG/S and NGS-2/S cathodes during 20 cycles. The TRG/S electrode showed a gradual decrease in the intensity of the cathodic and anodic peaks. In comparison to the TRG/S cathode, the NGS-2/S electrode exhibited more stable curve overlap that confirmed the high reversibility and stability of the electrode. From this result, it was thought that the N-doped graphene electrode showed a stable redox reaction of sulfur due to the limited dissolution of the polysulfide or limited desertion from the electrode.

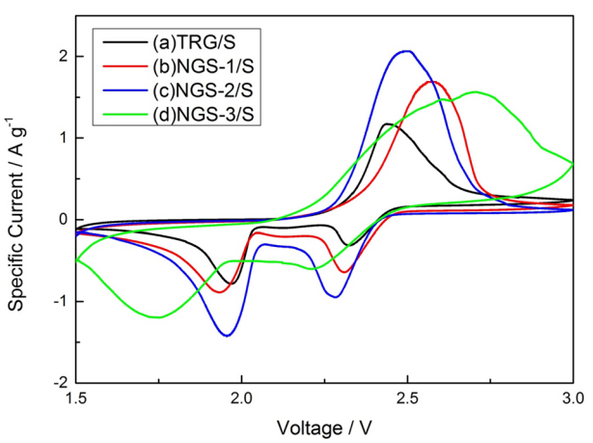

Fig. 3. Cycle voltammetry plots of TRG/S, NGS-1/S, NGS-2/S, and NGS-3/S electrodes at 0.2 mVs^{-1} for the first cycle. TRG, thermally reduced graphene; NGS, nitrogen-doped graphene sheets.

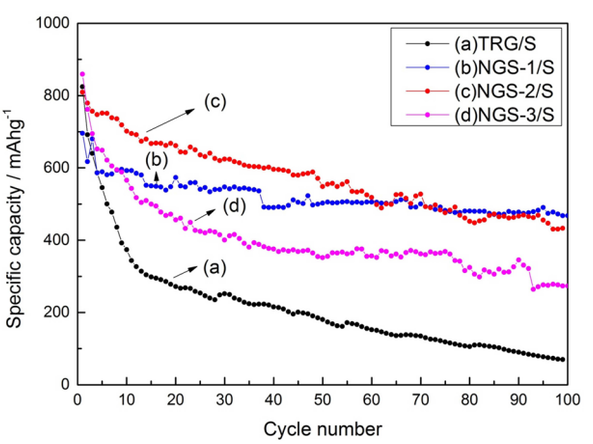

Fig. 5. Cycle performance of TRG/S, NGS-1/S, NGS-2/S, and NGS-3/S electrodes at 100 mAh g^{-1}. TRG, thermally reduced graphene; NGS, nitrogen-doped graphene sheets.

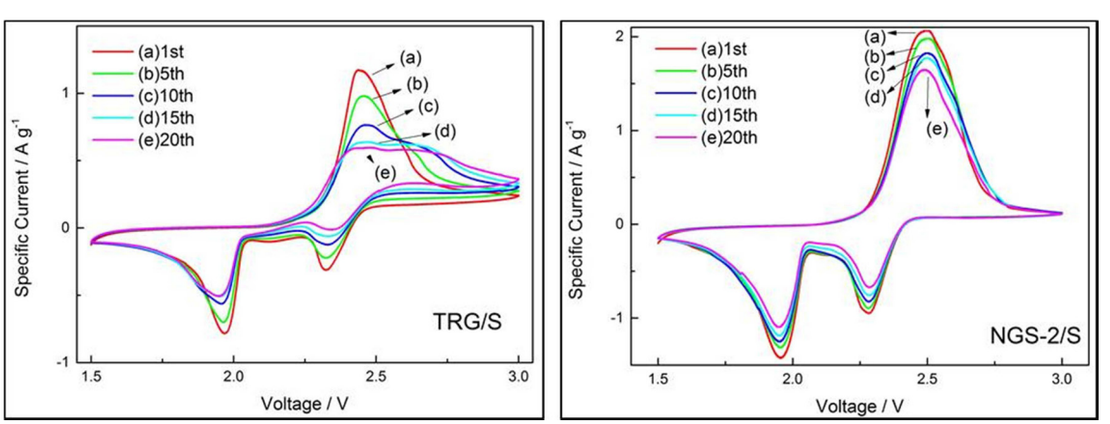

Fig. 4. Cyclic voltammetry plots of TRG/S and NGS-2/S electrodes at 0.2 mVs^{-1} for 20 cycles. TRG, thermally reduced graphene; NGS, nitrogen-doped graphene sheets.

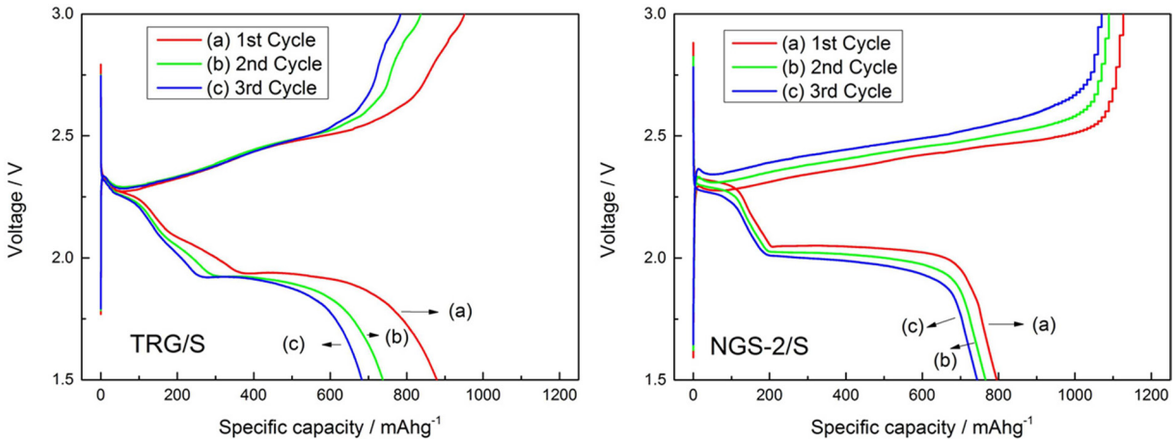

Fig. 6. Charge-discharge profiles of TRG/S and NGS-2/S electrodes at 100 mAh g^{-1} for the first three cycles. TRG, thermally reduced graphene; NGS, nitrogen-doped graphene sheets.

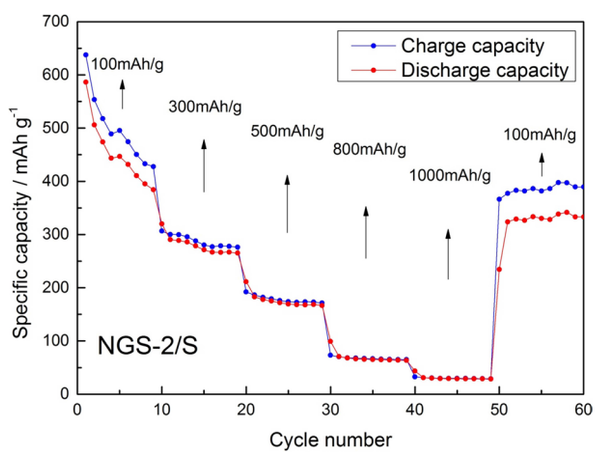

Fig. 7. Rate capability of a NGS-2/S electrode at rates from 100 to 1000 mAh g^{-1}. NGS, nitrogen-doped graphene sheets.

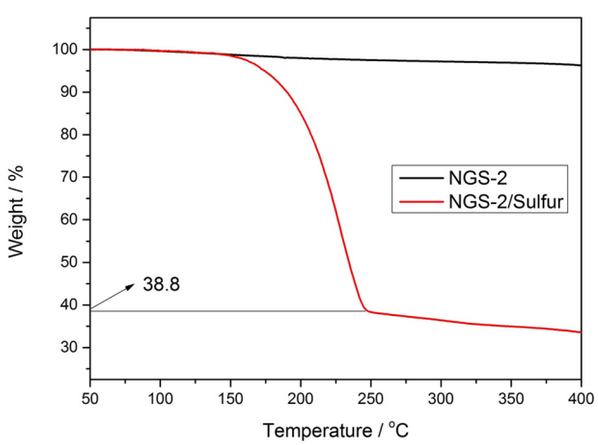

Fig. 8. Thermogravimetric analysis curves of the NGS-2 and NGS-2/S composites in nitrogen gas. NGS, nitrogen-doped graphene sheets.

The cycle performances of all the cathodes at 100 mAh g^{-1} are shown in Fig. 5. All the composite electrodes showed similar initial capacity (~800 mAh g^{-1}) but the TRG/S cathode showed a rapid decrease of capacity over 100 cycles. In contrast, the nitrogen-doped graphene cathodes maintained their specific capacity after 100 cycles. The change in the discharge capacity during 100 cycles, of TRG/S and NGS-2/S cathodes, was 824 to 70 mAh g^{-1} and 809 to 433 mAh g^{-1}, respectively. Regarding the NGS-1/S cathode, the specific capacity was slightly lower than that of the NGS-2/S cathode during the initial cycles. But after 50 cycles, the NGS-1/S cathode showed a specific capacity similar to that of the NGS-2/S cathode. The NGS-3/S cathode showed higher specific capacity than did the TRG/S cathode, but was definitely lower than the NGS-1/S and NGS-2/S cathodes. This means that excessive nitrogen atoms in the carbon matrix of graphene caused poor electrochemical performance, or low utilization of the sulfur reaction.

Fig. 6a and b are the charge-discharge profiles of TRG/S and NGS-2/S cathodes, respectively, at 100 mAh g^{-1} during

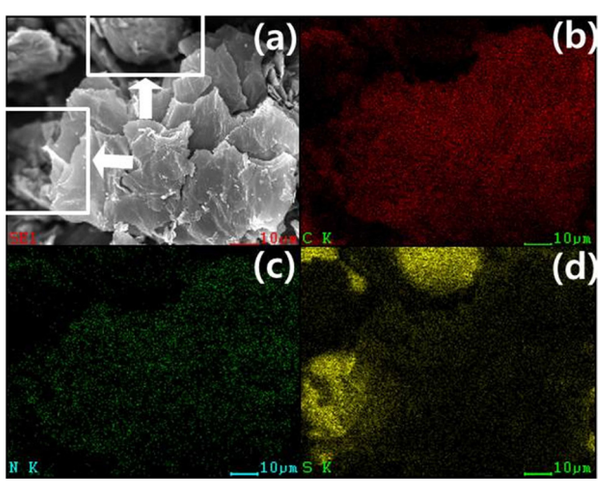

Fig. 9. (a) Field emission scanning electron microscope images and (b-d) elemental X-ray mapping of NGS-2/S composite. NGS, nitrogen-doped graphene sheets.

DOI: http://dx.doi.org/10.5714/CL.2016.19.040

the first three cycles. In both cathodes, two discharge plateaus can be distinguished in the voltage ranges of 2.2–2.4 V and 1.8–2.0 V. The first plateau corresponds to the formation of long chain polysulfides (Li_2S_X, $4 \leq X \leq 8$), and the second plateau to formation of short chain Li_2S_2 or Li_2S [29]. The second plateau is relatively longer than the first, which means that the discharge capacity is contributed by the second step of reduction. All of the redox plateaus are consistent with peaks of the CV curves. In addition, the potential plateaus of the NGS-2/S cathode are more stable and distinct than for the TRG/S cathode during the first three cycles. This means that the nitrogen doping enhances the electrochemical properties of lithium sulfur cells.

The rate capability of the NGS-2/S cathode at different rates was tested and results presented in Fig. 7. As the rates were gradually increased from 100 to 1000 mAh g^{-1}, the discharge capacity decreased. When the current rate returned to 100 mAh g^{-1} the capacity of the NGS-2/S cathode recovered to 323 mAh g^{-1}, equal to the capacity of the last cycle (100 mAh g^{-1}). The recovery ability of a cathode indicates a stable structure and tolerance to varying current density.

The sulfur loading of NGS-2/S composite, which showed the highest capacity, was determined by TGA. TGA (Fig. 8) shows 61.2% of sulfur loading in NGS-2/S composite, and this high sulfur content could be what provides the high overall energy density per unit mass of the cathode in Li-S cells.

The morphology and microstructure of the NGS-2/S composite were investigated using FE-SEM. Fig. 9a shows a typical 2-dimensional plate-like structure of graphene, and a sulfur particle is indicated by an arrow. Elemental X-ray mapping (Fig. 9b-d) showed homogeneous distribution of carbon, nitrogen, and sulfur in the NGS/S composites.

4. Conclusions

In summary, NGS with sulfur loading as high as 61.2 wt% were simply synthesized using a thermal solid-state reaction. Elemental sulfur immobilized within NGS sheets was fabricated using a solution-based preparation method, followed by a melt-diffusion technique. Nitrogen doping could assist graphene in suppressing the diffusion of polysulfide by enhancing its adsorption by surface modification. The NGS-2/S cathode, which contains 16.43 at% of nitrogen, in particular, shows enhanced reversibility of the sulfur redox reaction and the best cycle stability over 100 cycles. From the electrochemical characterization by CV test, and the galvanostatic charge/discharge tests, the NGS/S cathodes showed superior reversibility and cycle stability for 100 cycles over the pristine reduced GO/S cathode. These results demonstrate that nitrogen doping of modified GO supports, improve not only the sulfur-reaction stability but also the characteristics providing longer cycling.

Conflict of Interest

No potential conflict of interest relevant to this article was reported.

Acknowledgments

This work was supported by the Individual Basic Science & Engineering Research Program through the National Research Foundation of Korea (Grant No. NRF-2015R1D1A1A01060822), funded by the Ministry of Education, Republic of Korea.

References

[1] Manthiram A, Fu Y, Chung SH, Zu C, Su YS. Rechargeable lithium-sulfur batteries. Chem Rev, **114**, 11751 (2014). http://dx.doi.org/10.1021/cr500062v.

[2] Kim S, Hwang EJ, Jung Y, Han M, Park SJ. Ionic conductivity of polymeric nanocomposites electrolytes based on poly(ethylene oxide) and organo-clay materials. Colloids Surf A: Physicochem Eng Aspects, **313-314**, 216 (2008). http://dx.doi.org/10.1016/j.colsurfa.2007.04.097.

[3] Oh M, Kim S. Effect of dodecyl benzene sulfonic acid on the preparation of polyaniline/activated carbon composites by in situ emulsion polymerization. Electrochim Acta, **59**, 196 (2012). http://dx.doi.org/10.1016/j.electacta.2011.10.058.

[4] Ji X, Nazar LF. Advances in Li-S batteries. J Mater Chem, **20**, 9821 (2010). http://dx.doi.org/10.1039/B925751A.

[5] Wang JZ, Lu L, Choucair M, Stride JA, Xu X, Liu HK. Sulfur-graphene composite for rechargeable lithium batteries. J Power Sources, **196**, 7030 (2011). http://dx.doi.org/10.1016/j.jpowsour.2010.09.106.

[6] Cao Y, Li X, Aksay IA, Lemmon J, Nie Z, Yang Z, Liu J. Sandwich-type functionalized graphene sheet-sulfur nanocomposite for rechargeable lithium batteries. Phys Chem Chem Phys, **13**, 7660 (2011). http://dx.doi.org/ 10.1039/C0CP02477E.

[7] Thieme S, Brückner J, Meier A, Bauer I, Gruber K, Kaspar J, Helmer A, Althues H, Schmuck M, Kaskel S. A lithium–sulfur full cell with ultralong cycle life: influence of cathode structure and polysulfide additive. J Mater Chem A, **3**, 3808 (2015). http://dx.doi.org/ 10.1039/C4TA06748G.

[8] Zhang W, Qiao D, Pan J, Cao Y, Yang H, Ai X. A Li+ -conductive microporous carbon-sulfur composite for Li-S batteries. Electrochim Acta, **87**, 497 (2013). http://dx.doi.org/10.1016/j.electacta.2012.09.086.

[9] Zhang SS, Read JA. A new direction for the performance improvement of rechargeable lithium/sulfur batteries. J Power Sources, **200**, 77 (2012). http://dx.doi.org/10.1016/j.jpowsour.2011.10.076.

[10] Chung SH, Singhal R, Kalra V, Manthiram A. Porous carbon mat as an electrochemical testing platform for investigating the polysulfide retention of various cathode configurations in Li-S cells. J Phys Chem Lett, **6**, 2163 (2015). http://dx.doi.org/ 10.1021/acs.jpclett.5b00927.

[11] Li J, Li L, Zhang B, Yu M, Ma H, Zhang J, Zhang C, Li J. Synthesis of few-layer reduced graphene oxide for lithium-ion battery electrode materials. Ind Eng Chem Res, **53**, 13348 (2014). http://dx.doi.org/ 10.1021/ie5018282.

[12] Park JY, Kim S. Preparation and electroactivity of polymer-functionalized graphene oxide-supported platinum nanoparticles catalysts. Int J Hydrogen Energy, **14**, 6275 (2013). http://dx.doi.org/10.1016/j.ijhydene.2012.12.059.

[13] Raccichini R, Varzi A, Passerini S, Scrosati B. The role of graphene

for electrochemical energy storage. Nat Mater, **14**, 271 (2015). http://dx.doi.org/10.1038/nmat4170.

[14] Ju HM, Huh SH, Choi SH, Lee HL. Structures of thermally and chemically reduced graphene. Mater Lett, **64**, 357 (2010). http://dx.doi.org/10.1016/j.matlet.2009.11.016.

[15] Kim J, Kim S. Preparation and electrochemical property of ionic liquid-attached graphene nanosheets for an application of supercapacitor electrode. Electrochim Acta, **119**, 11 (2014). http://dx.doi.org/10.1016/j.electacta.2013.11.187.

[16] Wakeland S, Martinez R, Grey JK, Luhrs CC. Production of graphene from graphite oxide using urea as expansion–reduction agent. Carbon, **48**, 3463 (2010). http://dx.doi.org/10.1016/j.carbon.2010.05.043.

[17] Sun L, Wang L, Tian C, Tan T, Xie Y, Shi K, Li M, Fu H. Nitrogen-doped graphene with high nitrogen level via a one-step hydrothermal reaction of graphene oxide with urea for superior capacitive energy storage. RCS Adv, **2**, 4498 (2012). http://dx.doi.org/10.1039/C2RA01367C.

[18] Wang X, Zhang Z, Qu Y, Lai Y, Li J. Nitrogen-doped graphene/sulfur composite as cathode material for high capacity lithium–sulfur batteries. J Power Sources, **256**, 361 (2014). http://dx.doi.org/10.1016/j.jpowsour.2014.01.093.

[19] Mou Z, Chen X, Du Y, Wang X, Yang P, Wang S. Forming mechanism of nitrogen doped graphene prepared by thermal solid-state reaction of graphite oxide and urea. Appl Surf Sci, **258**, 1704 (2011). http://dx.doi.org/10.1016/j.apsusc.2011.10.019.

[20] Tao L, Dou S, Ma Z, Shen A, Wang S. Simultaneous Pt deposition and nitrogen doping of graphene as efficient and durable electrocatalysts for methanol oxidation. Int J Hydrogen Energy, **40**, 14371 (2015). http://dx.doi.org/10.1016/j.ijhydene.2015.02.104.

[21] Wang C, Chen H, Dong W, Ge J, Lu W, Wu X, Guo L, Chen L. Sulfur-amine chemistry-based synthesis of multi-walled carbon nanotube-sulfur composites for high performance Li-S batteries. Chem Commun, **50**, 1202 (2014). http://dx.doi.org/ 10.1039/C3CC47223J.

[22] Xu X, Yuan T, Zhou Y, Li Y, Lu J, Tian X, Wang D, Wang J. Facile synthesis of boron and nitrogen-doped graphene as efficient electrocatalyst for the oxygen reduction reaction in alkaline media. Int J Hydrogen Energy, **39**, 16043 (2014). http://dx.doi.org/10.1016/j.ijhydene.2013.12.079.

[23] Lin Z, Waller G, Liu Y, Liu M, Wong CP. Facile synthesis of nitrogen-doped graphene via pyrolysis of graphene oxide and urea, and its electrocatalytic activity toward the oxygen-reduction reaction. Adv Energy Mater, **2**, 884 (2012). http://dx.doi.org/10.1002/aenm.201200038.

[24] Sun F, Wang J, Chen H, Li W, Qiao W, Long D, Ling L. High efficiency immobilization of sulfur on nitrogen-enriched mesoporous carbons for Li-S batteries. ACS Appl Mater Interfaces, **5**, 5630 (2013). http://dx.doi.org/10.1021/am400958x.

[25] Kim S, Park SJ. Electrical signal effect on electrochemical activities of metal catalysts electrically deposited on carbon nanotubes. Electrochim Acta, **53**, 4082 (2008). http://dx.doi.org/10.1016/j.electacta.2007.08.067.

[26] Azimi N, Xue Z, Hu L, Takoudis C, Zhang S, Zhang Z. Additive effect on the electrochemical performance of lithium-sulfur battery. Electrochim Acta, **154**, 205 (2015). http://dx.doi.org/10.1016/j.electacta.2014.12.041.

[27] Ji X, Lee KT, Nazar LF. A highly ordered nanostructured carbon–sulphur cathode for lithium–sulphur batteries. Nat Mater, **8**, 500 (2009). http://dx.doi.org/10.1038/nmat2460.

[28] Kim S, Jung Y, Park SJ. Effect of imidazolium cation on cycle life characteristics of secondary lithium–sulfur cells using liquid electrolytes. Electrochim Acta, **52**, 2116 (2007). http://dx.doi.org/10.1016/j.electacta.2006.08.028.

[29] Ji L, Rao M, Zheng H, Zhang L, Li Y, Duan W, Guo J, Cairns EJ, Zhang Y. Graphene oxide as a sulfur immobilizer in high performance lithium/sulfur cells. J Am Chem Soc, **133**, 18522 (2011). http://dx.doi.org/ 10.1021/ja206955k.